

Correlation between the valence state of cerium and the magnetic transition in $\text{Ce}(\text{Ru}_{1-x}\text{Fe}_x)_2\text{Al}_{10}$ studied by resonant x-ray emission spectroscopy

Yumiko Zekko,¹ Yoshiya Yamamoto,¹ Hitoshi Yamaoka,² Fumisato Tajima,³ Takashi Nishioka,³ Fabio Strigari,⁴ Andrea Severing,⁴ Jun-Fu Lin,⁵ Nozomu Hiraoka,⁶ Hirofumi Ishii,⁶ Ku-Ding Tsuei,⁶ and Jun'ichiro Mizuki¹

¹Graduate School of Science and Technology, Kwansai Gakuin University, Sanda, Hyogo 669-1337, Japan

²RIKEN SPring-8 Center, RIKEN, 1-1-1 Kouto, Mikazuki, Sayo, Hyogo 679-5148, Japan

³Graduate School of Integrated Arts and Sciences, Kochi University, 2-5-1 Akebono, Kochi 780-8520, Japan

⁴Institute of Physics II, University of Cologne, Zùlpicher Straße 77, 50937 Cologne, Germany

⁵Department of Geological Sciences, The University of Texas at Austin, Austin, Texas 78712, USA

⁶National Synchrotron Radiation Research Center, Hsinchu 30076, Taiwan

(Received 26 December 2013; revised manuscript received 17 February 2014; published 12 March 2014)

The correlation between the $4f$ -conduction electron (c - f) hybridization and the transition temperature T_0 into the unconventional antiferromagnetically (AFM) ordered state in $\text{Ce}(\text{Ru}_{1-x}\text{Fe}_x)_2\text{Al}_{10}$ has been investigated. The impact of pressure on the crystal structure and the electronic structure has been measured using x-ray diffraction and resonant x-ray emission spectroscopy at the Ce L_3 absorption edge in a diamond anvil cell. Our results show that the lattice spacings imply some correlation with the disappearance of T_0 . Analyses of the measured valence states, however, show only a weak correlation with the corresponding critical disappearance of the AFM order within experimental errors. Our results may be explained by a scenario based on the Kondo-Heisenberg model beyond the conventional Doniach phase diagram.

DOI: 10.1103/PhysRevB.89.125108

PACS number(s): 71.27.+a, 74.62.Fj, 75.30.Mb, 78.70.En

The nature of the itinerant-localized transition of heavy electrons has been studied in the last few decades as an outstanding problem in the strongly correlated electron systems. Localized f electrons tend to form magnetically ordered states with an exchange interaction, while the itinerant character arises from the Kondo effect with a spin singlet that results in a heavy Fermi liquid. Unconventional phenomena have often been observed near the quantum critical point where the itinerant and localized character competes. The Doniach model has been used to describe the phase diagram of the system in terms of a competition between a local moment exchange represented by the Ruderman-Kittel-Kasuya-Yosida (RKKY) interaction and the Kondo screening [1,2]. However, recent theoretical results have indicated that the Doniach model is too simple to describe the exotic phenomena in many relevant systems [3,4]. In this paper our experimental results show a possible scenario for the breakdown of the conventional picture of the competition between the RKKY interaction and Kondo effect in $f + d$ electron systems.

Recently it was found that in $\text{CeT}_2\text{Al}_{10}$ antiferromagnetic (AFM) order appears for $T = \text{Ru}$ and Os at unusually high ordering temperatures ($T_0 = 27.3$ and 28.7 K) with fairly small ordered moments of $\mu_{\text{ord}} \approx 0.40$ and $0.29 \mu_B/\text{Ce}$ for $T = \text{Ru}$ and Os , respectively [5–7]. $\text{CeFe}_2\text{Al}_{10}$ shows semiconducting behavior at low temperatures and does not exhibit magnetic order. Its temperature dependence rather suggests intermediate valent behavior due to hybridization of $4f$ and conduction electrons (c - f) [6,8–12].

The size of the small ordered moments in the Ru and Os compounds along the c direction and the anisotropy of the magnetic properties ($\chi_a > \chi_c > \chi_b$) in the paramagnetic state [6,13–15] can be explained to a large extent by crystal-field effects (CEF) [16,17]. However, the direction of the ordered moments comes as a surprise since it is aligned along the c axis and not along the easy axis a . The long Ce-Ce distances of $> 5 \text{ \AA}$ in $\text{CeRu}_2\text{Al}_{10}$ and $\text{CeOs}_2\text{Al}_{10}$ and de-Gennes

scaling imply ordering temperatures below a few K, so that conventional RKKY interaction can be ruled out as the origin of the magnetic order [18]. Anisotropic exchange interaction was considered to reproduce the AFM ordering temperature, but the magnetic behavior at $T < T_0$ cannot be explained within a mean-field approximation, even when taking into account the CEF effects [19]. Therefore, the suppression of the spin degrees of freedom due to the c - f hybridization was considered. It was suggested that the c - f hybridization is strongest along the a axis, leading to an easy magnetization axis in the c direction [14].

The reason why T_0 is so anomalously large remains an unresolved problem. Usually the Kondo effect, i.e., the presence of c - f hybridization, suppresses the magnetic order. We therefore study systematically what impact the Kondo effect has on the transition temperature T_0 . A measure for the c - f hybridization is the cerium valence which can be obtained from deviations of the lattice distances from Vegard's law, or more directly, from the electronic occupation of the $4f$ shell. The hybridization can be varied by pressure, chemically or hydrostatically. For the application of chemical pressure we have chosen to replace the transition metal in $\text{CeRu}_2\text{Al}_{10}$ with Fe. The magnetic order has disappeared between $x = 0.7$ and 0.8 [20,21]. Applying hydrostatic pressure to $\text{CeRu}_2\text{Al}_{10}$ leads at first to an increase of T_0 , then, after passing a maximum at 2 GPa, to a decrease and sudden disappearance of the magnetic transition at 4 GPa [22].

In this paper we present x-ray diffraction (XRD) results of the lattice parameters and atomic distances in $\text{Ce}(\text{Ru}_{1-x}\text{Fe}_x)_2\text{Al}_{10}$ at 300 K. Then we show valence measurements with the bulk sensitive x-ray absorption (XAS) technique with partial fluorescence yield (PFY) mode at the Ce L_3 absorption edge. We have used the PFY-XAS method where a decay process with longer life time is selected, so that the resulting spectra are narrower, making the different $4f$ contributions more visible [23]. Electronic structures of

$\text{Ce}(\text{Ru}_{1-x}\text{Fe}_x)_2\text{Al}_{10}$ as a function of x and that of $\text{CeRu}_2\text{Al}_{10}$ as a function of pressure at low temperatures have been measured. Our results show poor correlation between the change in the Ce valence and the sudden disappearance of T_0 in both x and pressure dependencies, seemingly supporting a theoretical scenario proposed recently [4].

Single crystals of $\text{Ce}(\text{Ru}_{1-x}\text{Fe}_x)_2\text{Al}_{10}$ ($x = 0, 0.125, 0.25, 0.375, 0.5, 0.6, 0.75, 0.8, 0.875, \text{ and } 1.0$) were synthesized by a conventional Al self-flux method. PFY-XAS and RXES measurements were performed at the Taiwan beamline BL12XU at SPring-8 [23]. A diamond anvil cell was used for the high pressure experiments. An ethanol-methanol mixture was loaded into a sample chamber hole of the Be gasket as the pressure medium. Pressure was monitored using ruby fluorescence, which was calibrated with an empirical formula at low temperatures [24].

The composition (x) dependence of the crystal structure was studied by XRD for $\text{Ce}(\text{Ru}_{1-x}\text{Fe}_x)_2\text{Al}_{10}$ at 300 K. Figures 1(a) and 1(b) show the changes in the lattice constants and in the volume as a function of x . On the whole our

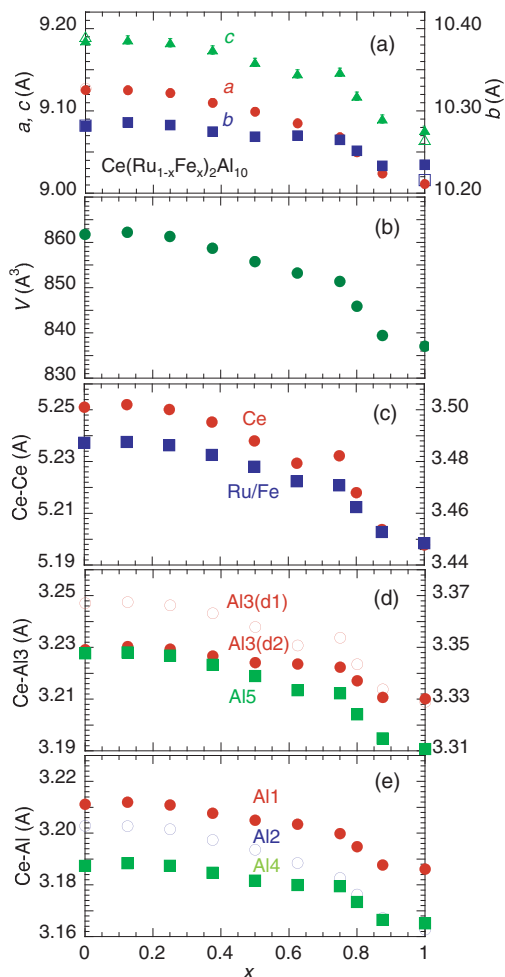


FIG. 1. (Color online) (a) Change in the orthorhombic lattice parameters of a , b , and c as a function of x for $\text{Ce}(\text{Ru}_{1-x}\text{Fe}_x)_2\text{Al}_{10}$ ($x = 0$ to 1.0) at 300 K. (b) Change in the volume as a function of x . Data errors are comparable to the symbol sizes. (c)–(e) Interatomic distance as a function of x for $\text{Ce}(\text{Ru}_{1-x}\text{Fe}_x)_2\text{Al}_{10}$.

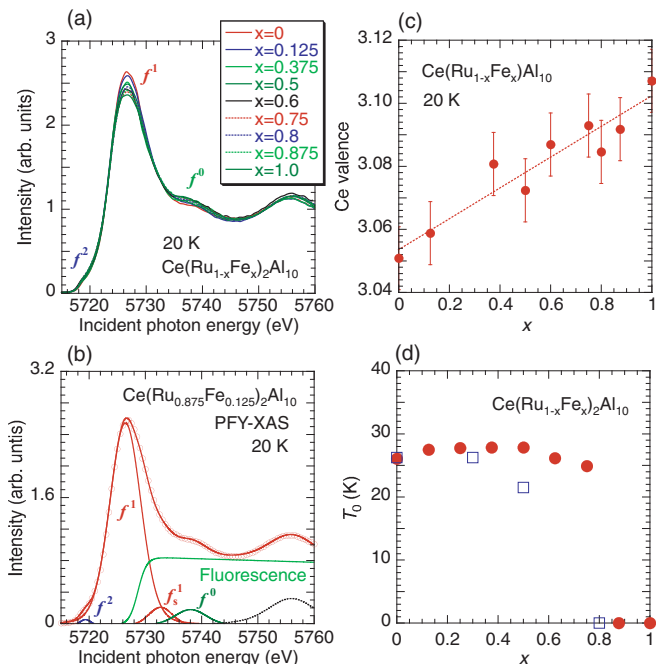


FIG. 2. (Color online) (a) x dependence of the PFY-XAS spectra at 20 K for $\text{Ce}(\text{Ru}_{1-x}\text{Fe}_x)_2\text{Al}_{10}$. (b) x dependence of the Ce valence derived from the PFY-XAS spectra. (c) An example of the fit to the PFY-XAS spectra (open circles) measured at 20 K for $\text{Ce}(\text{Ru}_{0.875}\text{Fe}_{0.125})_2\text{Al}_{10}$. Dotted line is a guide for the eye fitted with linear function. (d) x dependence of the Néel temperature (T_0) for $\text{CeRu}_2\text{Al}_{10}$. The data in (d) are taken from the results of the susceptibility [20] (closed circle) and μSR [21] (open square) measured previously.

results agree with neutron diffraction studies by Adroja *et al.* who observed a weak deviation from a linear decrease of the unit cell volume from $\text{CeRu}_2\text{Al}_{10}$ to $\text{CeFe}_2\text{Al}_{10}$ for the $x = 0.8$ and 1.0 samples with the five compositions of x [21]. But we find that our detailed XRD data yield a gradual decrease of the lattice constants and volume between $x = 0$ and 0.6 and a more rapid decrease above $x = 0.75$. The same trend is observed in the interatomic distances Ce-Ce, Ce-(Ru, Fe), and Ce-Al as shown in Figs. 1(c)–1(e). Interestingly, the change in the angle among Ce-Al-Ce atoms shows that the alignment of Ce-Al1-Ce is nearly rectilinear and does not show the x dependence, while those of Ce-Al3-Ce and Ce-Al5-Ce show an opposite trend and change rapidly at $x > 0.5$ – 0.6 [25].

In Fig. 2(a) the PFY-XAS spectra of $\text{Ce}(\text{Ru}_{1-x}\text{Fe}_x)_2\text{Al}_{10}$ at 20 K are shown for all compositions. The intensities have been normalized to the spectral areas in the measured energy range from 5710 to 5760 eV. These spectra show the presence of c - f hybridization because in addition to the dominating absorption edge due to f^1 (Ce^{3+}) in the ground state, additional absorption features due to small fractions of f^2 (Ce^{2+}) and f^0 (Ce^{4+}) are visible. We observe that with increasing Fe concentration x the f^1 component decreases, whereas that of the f^0 contribution increases. The f^2 component changes only very little. In these measurements, we observe the $\text{Ce } 3d_{3/2} \rightarrow 2p_{3/2}$ deexcitation following a $2p_{3/2} \rightarrow 5d$ excitation. Thus the final state includes a $3d$ core-hole, which can cause a

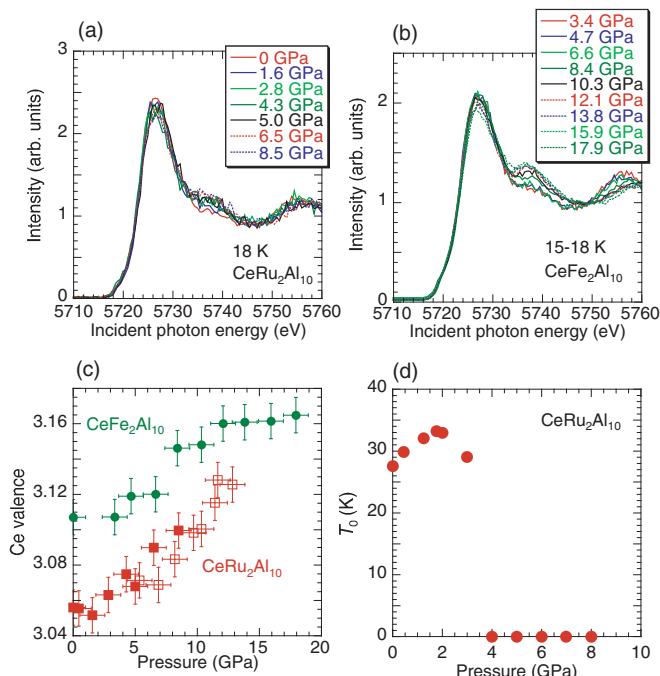


FIG. 3. (Color online) (a) Pressure dependence of the PFY-XAS spectra at 18 K for CeRu₂Al₁₀. (b) Pressure dependence of the PFY-XAS spectra at 15–18 K for CeFe₂Al₁₀. (c) Pressure dependence of the Ce valence for CeRu₂Al₁₀ and CeFe₂Al₁₀ derived from the fits to the PFY-XAS spectra. Symbols of open and closed squares for CeRu₂Al₁₀ correspond to different series of the measurements. (d) Pressure dependence of the Néel temperature (T_0) for CeRu₂Al₁₀ [22].

dynamic screening effect by the core-hole potential in the final excited state [25,26]. For simplicity in this paper we treat v as the mean Ce valence.

In Fig. 2(b) we show the fit to the PFY-XAS data of Ce(Ru_{0.875}Fe_{0.125})₂Al₁₀ at 20 K as an example. For simplicity the f^n components are described with Voigt profiles although the spectral shape is more complicated due to band effects [27]. For the fluorescence an arctanlike function was assumed. For a proper fit of the $4f^1$ feature two lines, the main f^1 line and a weak satellite f_s^1 were taken into account. However, all data were fitted in the same manner so that a trend in the spectrum as a function of x from such a fit was able to be obtained. Figure 3(c) shows the Ce valence derived from these fits to the PFY-XAS spectra as a function of x . The valence of 3.05 ± 0.01 of CeRu₂Al₁₀ agrees well with PES measurements by Goraus *et al.* [28]. We further find that the Ce valence increases linearly with x within the error bars. We also took RXES spectra as a function of incident photon energies for the compositions close to the disappearance of magnetic order ($x = 0.60, 0.75, \text{ and } 0.875$), confirming very small difference of the electronic structures of these compounds [25]. We measured the pressure dependence of the PFY-XAS spectra at 15–18 K for CeT₂Al₁₀ ($T = \text{Ru, Fe}$) as shown in Figs. 3(a) and 3(b). For the Ru compound the maximum pressure was 8.5 GPa, while for the Fe compound it was 17.9 GPa. The data statistics are less optimal than for the data shown in Fig. 3(a) due to the low count rate in the

DAC. Nevertheless, we observed the trend that with increasing pressure the f^0 intensity increases while the f^1 contribution decreases. Figure 3(c) shows the Ce valence derived from the fits to the PFY-XAS spectra. We find a monotonically increasing valence. No particular valence transition as a function of pressure occurs within the experimental errors. Up to 8.5 GPa the valence change with pressure is similar for CeFe₂Al₁₀ and CeRu₂Al₁₀. Above 12 GPa the Ce valence for CeFe₂Al₁₀ changes while pressure flattens out. These findings are consistent with the absence of any pressure-induced volume changes [29].

The trend of the pressure-induced change in the Ce valence for CeRu₂Al₁₀ is similar to that for CeIrSi₃ [30] and CePd₂Si₂ [26], where a gradual valence change occurred from the Kondo region to the valence fluctuation region with pressure. In CeFe₂Al₁₀ similar behavior as in CeRu₂Al₁₀ is observed, but the change in the Ce valence is small above 12 GPa, where the transition from the Kondo to the valence fluctuation regions may occur as observed in Yb compounds [31,32]. Thus we conclude that CeRu₂Al₁₀ is not located in the valence fluctuation region but rather in the Kondo region at ambient pressure [26].

We find that already in the full compound CeRu₂Al₁₀ before the substitution a non-negligible amount of c - f hybridization is present. This indicates that the AFM state coexists with c - f hybridization. Kondo *et al.* has pointed out that the AFM moment along the c axis in the ordered state is not enough if it exists alone [14]. They proposed a scenario that the larger hybridization along the a axis could make a magnetization easy axis along the c axis. Interestingly, the LSDA + U band calculation showed that in CeRu₂Al₁₀ the magnetic configuration was unstable if Coulomb correlations among $4f$ electrons were not included [28]. This also indicates that the weak hybridization may stabilize the magnetic structure because the f - c Coulomb term correlates to the Ce valence. These results are consistent with our observation and we conclude that the weak c - f hybridization is favored to coexist with the magnetic order.

The lattice constants and atomic distances of Ce(Ru_{1-x}Fe_x)₂Al₁₀ have been measured as a function of x . We observe a rapid change in the lattice constants close to the composition where the AFM order is suppressed [20] [compare Fig. 1 and 3(d)]. In heavy fermion or intermediate valence systems valence changes go along with changes in the lattice constants due to the different ionic radii of the $4f^0$ and $4f^1$ states. We have further presented valence measurements with the PFY-XAS of the substitution series Ce(Ru_{1-x}Fe_x)₂Al₁₀ as a function of x . Our fits to the substitution series yield a smooth change in the valence which does not reflect the more rapid change as expected from the lattice constants beyond $x \approx 0.8$. Here we consider a relation between the changes in the volume and Ce valence. For an example, in the γ - α transition of Ce metal the change in the volume of 20% induces the change in the Ce valence of 0.16 at 2 GPa [33]. Although we cannot simply apply the result for the Ce metal to other Ce compounds, a few percent abrupt change in the volume may be necessary to observe a sudden change in the Ce valence. Our results show that the change in the volume of the order of 1%–2% around $x \sim 0.8$ does not change the electronic structure

significantly. The poor correlation between the change in the lattice and Ce valence is anomalous and at present it seems to indicate the breakdown of the RKKY scenario as an origin of the magnetic order as already seen in nonapplicability of the de-Gennes scaling for T_0 in $\text{CeT}_2\text{Al}_{10}$ systems ($T = \text{Ru, Os}$) [18].

In $\text{CeRu}_2\text{Al}_{10}$ T_0 increased initially to 2.5 GPa. The axial dependent resistivity (ρ) showed $\rho_b \sim \rho_c > \rho_a$ at ambient pressure and $\rho_b > \rho_c > \rho_a$ at 2.5 GPa [6,34]. Tanida *et al.* [34] proposed the following scenario: The c - f hybridization in the ac plane becomes large compared with that along the b axis with pressure and the slight increase of T_0 in low pressure range is ascribed to the enhancement of the c - f hybridization in the ac plane. In this scenario the RKKY-type interaction may be comparable to the Kondo effect at 2.5 GPa. In the pressure dependence of $\text{CeRu}_2\text{Al}_{10}$ the Ce valence shows a little change up to ~ 2 GPa while T_0 rises in between 0 and 2.5 GPa. Above ~ 2 GPa the Ce valence increases more rapidly in the pressure dependence. Thus the scenario proposed by Tanida *et al.* also explains our results at $P < 3$ –4 GPa. However, our pressure-induced behavior of the Ce valence in the whole pressure region measured has been often observed also in other Ce compounds, where the transition from the Kondo region to the valence fluctuation region occurs [26,30,35]. Furthermore, it is crucial that the sudden change in T_0 at $P > 3$ –4 GPa is beyond the above scenario because of the smooth change in the Ce valence.

We conclude, in $\text{CeRu}_2\text{Al}_{10}$ the anomalously high ordering temperatures in combination with c - f hybridization in the ordered state point towards a strong exchange interaction. It is therefore feasible that the Kondo effect has an impact on the ordered state such that it, e.g., influences the direction of the magnetic moment. Still, the conventional RKKY scenario does not yield an explanation for why the exchange interaction is so strong in these compounds and the sudden disappearance of the magnetic order in both x and pressure dependencies. Recently a new phase diagram of the itinerant-localized transition of heavy electrons has been clarified for the Kondo-Heisenberg lattice at finite temperatures [4]. $\text{CeRu}_2\text{Al}_{10}$ is located in the itinerant AFM region, while $\text{CeFe}_2\text{Al}_{10}$ is in the paramagnetic region. Phase transition occurs between them and Néel temperature rapidly goes down to zero around the phase transition point, but the Fermi temperature constantly increases. This picture is illustrated in Fig. 4(b) with a conventional Doniach phase diagram in Fig. 4(a). The theory indicates that even if the Heisenberg interaction is small compared to the Kondo term, it is still important because it competes with the Kondo energy. Substitution of Fe to the Ru site as well as to apply the pressure may cause the transition from the itinerant AFM to paramagnetic, while the hybridization strength changes gradually. Thus this theory may explain the experimental results for $\text{CeT}_2\text{Al}_{10}$ systems quantitatively. But further theoretical study is required for quantitative comparison with the experimental results.

Our data confirm that in $\text{CeRu}_2\text{Al}_{10}$ c - f hybridization is present at ambient pressure, i.e., the AFM state coexists with c - f hybridization. Pressure or Fe substitution to the Ru site pushes the system from a AFM ordered state to the valence fluctuation regime. The XRD study of the x dependence for $\text{Ce}(\text{Ru}_{1-x}\text{Fe}_x)_2\text{Al}_{10}$ indicates no structural

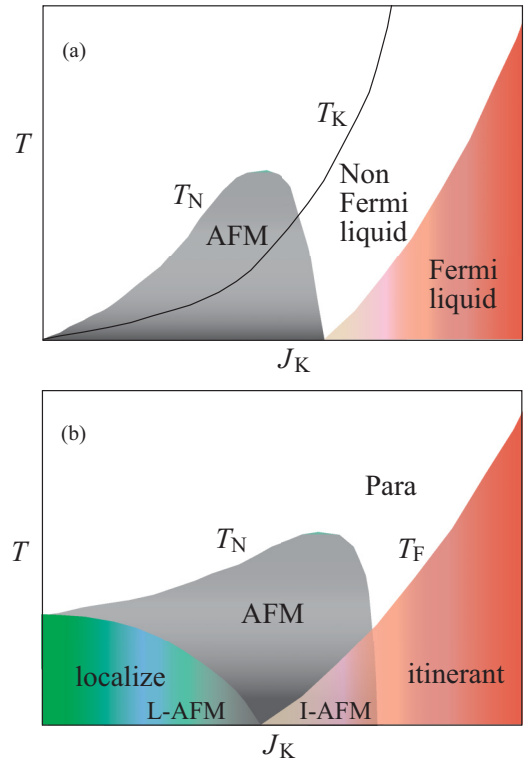


FIG. 4. (Color online) (a) Conventional Doniach phase diagram. There is a clear separation between the magnetically ordered state and the itinerant Fermi liquid [1]. (b) A phase diagram based on the calculation for the Kondo-Heisenberg lattice at finite temperatures [4].

transition, but a more rapid change in the volume close to $x \approx 0.8$, corresponding to the change in T_0 , suggests a change in Ce valence. While a smooth change of valence is also observed in the PFY-XAS data, we do not find that the valence reflects the sudden drop of the ordering temperature at neither $x \approx 0.8$ nor $P = 0.4$ GPa. Seemingly the c - f hybridization is not responsible for the strong enhancement of T_0 , although it has an impact on the magnetic structure. In our measurements we did not measure the orientation dependence of the crystal. It will be interesting to observe the orientation dependence especially in the x dependence.

The experiments were performed at Taiwan beamline BL12XU under SPring-8 Proposals No. 2012B4252, No. 2013A4251, and No. 2013A4255 (corresponding NSRRC Proposals No. 2012-3-013-1, No. 2012-3-013-2, and No. 2013-3-013-3). We are grateful to Satomi Kawase for her help in the experiment, and Naohito Tsujii and Akio Kotani for useful discussion. This work was partly supported by Grants in Aid for Scientific Research from the Japan Society for the Promotion of Science and the German funding agency DFG under Grant No. 600575. This work at UT Austin was supported as part of EFree, an Energy Frontier Research Center funded by the US Department of Energy Office of Science, Office of Basic Energy Sciences under Award DE-SC0001057. We also appreciate B. Shalab for editing the manuscript.

- [1] S. Doniach, *Physica B* **91**, 231 (1977).
- [2] B. Coqblin, M. D. Núñez-Regueiro, A. Theumann, J. R. Iglesias, and S. G. Magalhães, *Philos. Mag.* **86**, 2567 (2006).
- [3] H. Watanabe and M. Ogata, *Phys. Rev. Lett.* **99**, 136401 (2007).
- [4] S. Hoshino and Y. Kuramoto, *Phys. Rev. Lett.* **111**, 026401 (2013).
- [5] A. M. Strydom, *Physica B* **404**, 2981 (2009).
- [6] T. Nishioka, Y. Kawamura, T. Takesaka, R. Kobayashi, H. Kato, M. Matsumura, K. Kodama, K. Matsubayashi, and Y. Uwatoko, *J. Phys. Soc. Jpn.* **78**, 123705 (2009).
- [7] Y. Muro, J. Kajino, K. Umeo, K. Nishimoto, R. Tamura, and T. Takabatake, *Phys. Rev. B* **81**, 214401 (2010).
- [8] Y. Muro, K. Motoya, Y. Saiga, and T. Takabatake, *J. Phys. Soc. Jpn.* **78**, 083707 (2009).
- [9] Y. Muro, K. Motoya, Y. Saiga, and T. Takabatake, *J. Phys.: Conf. Ser.* **200**, 012136 (2010).
- [10] S. C. Chen and C. S. Lue, *Phys. Rev. B* **81**, 075113 (2010).
- [11] Y. Kawamura, S. Edamoto, T. Takesaka, T. Nishioka, H. Kato, M. Matsumura, Y. Tokunaga, S. Kambe, and H. Yasuoka, *J. Phys. Soc. Jpn.* **79**, 103701 (2010).
- [12] S.-I. Kimura, Y. Muro, and T. Takabatake, *J. Phys. Soc. Jpn.* **80**, 033702 (2011).
- [13] H. Tanida, D. Tanaka, M. Sera, C. Moriyoshi, Y. Kuroiwa, T. Takesaka, T. Nishioka, H. Kato, and M. Matsumura, *J. Phys. Soc. Jpn.* **79**, 043708 (2010).
- [14] A. Kondo, J. Wang, K. Kindo, Y. Ogane, Y. Kawamura, S. Tanimoto, T. Nishioka, D. Tanaka, H. Tanida, and M. Sera, *Phys. Rev. B* **83**, 180415 (2011).
- [15] K. Yutani, Y. Muro, J. Kajino, T. J. Sato, and T. Takabatake, *J. Phys.: Conf. Ser.* **391**, 012070 (2012).
- [16] F. Strigari, T. Willers, Y. Muro, K. Yutani, T. Takabatake, Z. Hu, Y.-Y. Chin, S. Agrestini, H.-J. Lin, C. T. Chen, A. Tanaka, M. W. Haverkort, L. H. Tjeng, and A. Severing, *Phys. Rev. B* **86**, 081105 (2012).
- [17] F. Strigari, T. Willers, Y. Muro, K. Yutani, T. Takabatake, Z. Hu, S. Agrestini, C.-Y. Kuo, Y.-Y. Chin, H.-J. Lin, T. W. Pi, C. T. Chen, E. Weschke, E. Schierle, A. Tanaka, M. W. Haverkort, L. H. Tjeng, and A. Severing, *Phys. Rev. B* **87**, 125119 (2013).
- [18] Y. Ogane, Y. Kawamura, T. Nishioka, H. Kato, M. Matsumura, Y. Yamamoto, K. Kodama, H. Tanida, and M. Sera, *J. Phys.: Conf. Ser.* **400**, 032073 (2012).
- [19] K. Kunimori, M. Nakamura, H. Nohara, H. Tanida, M. Sera, T. Nishioka, and M. Matsumura, *Phys. Rev. B* **86**, 245106 (2012).
- [20] T. Nishioka, D. Hirai, Y. Kawamura, H. Kato, M. Matsumura, H. Tanida, M. Sera, K. Matsubayashi, and Y. Uwaoko, *J. Phys.: Conf. Ser.* **273**, 012046 (2011).
- [21] D. T. Adroja, A. D. Hillier, Y. Muro, J. Kajino, T. Takabatake, P. Peratheepan, A. M. Strydom, P. P. Deen, F. Demmel, J. R. Stewart, J. W. Taylor, R. I. Smith, S. Ramos, and M. A. Adams, *Phys. Rev. B* **87**, 224415 (2013).
- [22] Y. Kawamura, Y. Ogane, T. Nishioka, H. Kato, M. Matsumura, K. Matsubayashi, and Y. Uwatoko, *J. Phys.: Conf. Ser.* **273**, 012038 (2011).
- [23] H. Yamaoka, I. Jarrige, N. Tsujii, J.-F. Lin, T. Ikeno, Y. Isikawa, K. Nishimura, R. Higashinaka, H. Sato, N. Hiraoka, H. Ishii, and K.-D. Tsuei, *Phys. Rev. Lett.* **107**, 177203 (2011).
- [24] Y. Feng, R. Jaramillo, J. Wang, Y. Ren, and T. F. Rosenbaum, *Rev. Sci. Instrum.* **81**, 041301 (2010).
- [25] See Supplemental Material at <http://link.aps.org/supplemental/10.1103/PhysRevB.89.125108> for the XRD results of the change in the angle among Ce-Al-Ce atoms. The RXES results as a function of incident photon energies are also shown for the $x = 0.60, 0.75$, and 0.875 samples.
- [26] H. Yamaoka, Y. Zekko, A. Kotani, I. Jarrige, N. Tsujii, J.-F. Lin, J. Mizuki, H. Abe, H. Kitazawa, N. Hiraoka, H. Ishii, and K.-D. Tsuei, *Phys. Rev. B* **86**, 235131 (2012).
- [27] F. Strigari *et al.* (unpublished).
- [28] J. Goraus and A. Ślebarski, *J. Phys.: Condens. Matter* **24**, 095503 (2012).
- [29] Y. Kawamura, K. Matsui, T. Kuwayama, T. Kawaai, S. Yamaguchi, Y. Nishijima, J. Hayashi, K. Takeda, and C. Sekine (unpublished).
- [30] H. Yamaoka, I. Jarrige, N. Tsujii, A. Kotani, J.-F. Lin, F. Honda, R. Settai, Y. Ōnuki, N. Hiraoka, H. Ishii, and K.-D. Tsuei, *J. Phys. Soc. Jpn.* **80**, 124701 (2011).
- [31] A. Fernandez-Pañella, V. Balédent, D. Braithwaite, L. Paolasini, R. Verbeni, G. Lapertot, and J.-P. Rueff, *Phys. Rev. B* **86**, 125104 (2012).
- [32] H. Yamaoka, N. Tsujii, Y. Utsumi, H. Sato, I. Jarrige, Y. Yamamoto, J.-F. Lin, N. Hiraoka, H. Ishii, K.-D. Tsuei, and J. Mizuki, *Phys. Rev. B* **87**, 205120 (2013).
- [33] J.-P. Rueff, J.-P. Itié, M. Taguchi, C. F. Hague, J.-M. Mariot, R. Delaunay, J.-P. Kappler, and N. Jaouen, *Phys. Rev. Lett.* **96**, 237403 (2006).
- [34] H. Tanida, Y. Nonaka, D. Tanaka, M. Sera, T. Nishioka, and M. Matsumura, *Phys. Rev. B* **86**, 085144 (2012).
- [35] H. Yamaoka, I. Jarrige, A. Ikeda-Ohno, S. Tsutsui, J.-F. Lin, N. Takeshita, K. Miyazawa, A. Iyo, H. Kito, H. Eisaki, N. Hiraoka, H. Ishii, and K.-D. Tsuei, *Phys. Rev. B* **82**, 125123 (2010).